IRSTI 532.5; 519.688 https://doi.org/10.26577/ijmph.2021.v12.i2.06

D.B. Zhakebayev[1,2], A.S. Zhumali[1,2], B.A. Satenova[2*]

[1]National Engineering Academy of the Republic of Kazakhstan, Almaty, Kazakhstan
[2]Al-Farabi Kazakh National University, Almaty, Kazakhstan
*e-mail: satenova.bekzat89@gmail.com

An Interpolated Bounce Back Thermable Method for Simulating Solid Particles Dynamics in a Viscous Medium

Abstract. In this paper we discuss the mathematical and computer modeling of non-isothermal two-phase flows with suspended particles. Natural convection between an outer cubical cavity and an inner hot sphere is investigated.

To simulate heat fluxes loaded with particles, a thermal model of the lattice Boltzmann equation in combination with the interpolated bounce back method (TLBM-IBB) has been developed. In TLBM-IBB, IBB is used to process liquid-solid interfaces, and TLBM is used to simulate the heat flow of a fluid. The momentum exchange method is used to calculate the hydrodynamic force on the particle surface. Simulation performed for a range of Rayleigh numbers $(10^5 - 10^6)$.

The accuracy and efficiency of the existing method is demonstrated by the example of solving the test problem of natural convection around a stationary particle and three-dimensional compressible natural convection in a square cavity filled with air, which has a hot wall on the left and a cold wall on the right, and two horizontal walls are adiabatic. The results obtained are in good agreement with the experimental and numerical results of other authors.

Key words: TLBM, IBB, D3Q19, solid particle, cubical cavity, viscous medium.

Introduction

Dispersed multiphase flows are widespread in nature and industry. In such applications, the movement of solid particles is often accompanied by heat transfer phenomena and chemical reactions. Moreover, particle motion and heat transfer between carrier fluid and particles in these thermomechanical systems are often strongly interrelated. In these cases, heat transfer dominates and controls the flow, creating natural convection currents and counter-currents, modifying locally the fluid viscosity, etc. With the rapid development of computer power, direct numerical simulation (DNS) based on the Navier-Stokes equations or the discrete lattice Boltzmann equation for solving fluid flow problems has become a practical and important tool for studying mechanics in solid particle flows. Many DNS methods have been proposed over the past decade. They can be divided into two categories: Boundary Fitting Methods and No Boundary Fitting Methods, depending on whether a bounding mesh is used to solve the flow field. For boundary fitting methods, such as the finite element method of arbitrary Lagrangian-Eulerian (ALE) (FEM) [1], fluid flow is calculated on a mesh with boundary fitting, and usually re-engagement is required as the interface moves, while for methods without boundary approximations such as the Lattice Boltzmann Method (LBM) [2], the Immersed Boundary Method (IB) [3], the Lagrange Distributed Multiplier Method (DLM / FD) [4], Accelerated Stokes Dynamics (ASD) [5] and the force interaction method (FCM) [6,7], the fluid flow is calculated on a stationary grid built over the entire area, including both the outer and inner parts of the particles. Although there has been an increasing interest for corresponding studies in recent years, only few publications can be found.

Mesoscopic methods solve a relatively simple basic equation and have definite properties, such as low numerical dissipation, the possibility of processing complex boundaries and high parallel eff. Different kinetic models have been proposed for the treatment of thermal flow, excellent from Boussinesq, in which the work is considered at the expense of viscous dissipation and compression. Among these approaches, the model of the double distribution function is widely used when modeling the heat flow [8- 10].

Yu et al. [5] used the Distributed Lagrange Multiplier / Fictitious Domain (DLM / FDM) method to simulate two-dimensional (2D) heat transfer solid particle flows. They considered particles to be constant or variable temperature. Later, the DNS method based on the DLM / FD (Distributed Lagrange Multiplier / Fictitious Domain) method to

simulate the problem of a three-dimensional spherical catalyst rising in the body due to natural convection was proposed [4]. Later, various thermal TLBM models were proposed with a combination of the immersed boundary method for a more accurate representation of the real liquid-solid interface. Although each boundary processing scheme has been separately tested and applied to different physical problems, as far as we know, they have yet to be systematically compared and evaluated under the same conditions.

For example, in this work, the deposition of solid particles with thermal convection was simulated using the direct forcing IBM (immersed boundary method) – TLBM [2, 3]. At the same time, in the article [6], a method of high-order immersed boundaries was developed based on a ghost-cell (IBM) for flow and thermal modeling of multiphase flow systems with moving spherical particles. A Ström et al. applied the VOF (volume of fluid) method for the dynamics of the movement of solid particles in combination with the effects of heat transfer [1].

In this work, a thermal model of the lattice Boltzmann method with an interpolated bounce back scheme (IBB-TLBM) is developed to study the problem of natural convection with a curved surface. With this thermal LB model, we simulated the following two types of thermal flows: one is thermal flows in a cubic cavity with hot and cold vertical walls and located spherical particle with constant temperature, the other is natural convection in a cubic cavity convection between an outer cubical cavity and an inner hot spherical particle. For the numerical simulation of the problem the Lattice Boltzmann method applying the D3Q19 model is used.

Problem statement

To check the numerical algorithm, the results obtained within the framework of solving this problem were compared with the results obtained experimentally, which showed good agreement.

Two test problems are being solved in this work. In the first problem, the dynamics of a hot sphere in a closed cube-shaped cavity with top and bottom adiabatic walls and with the rest of the walls at zero temperature is considered (Figure 1, a). The center of the sphere is at a distance $m = \frac{L}{10}$ above the center of the cube. The proportion of the sphere diameter with the wall length is $\frac{D}{L} = \frac{2}{5}$.

Figure 1, b shows the computational domain of the second test problem, which concerns a dynamics of hot sphere, located in a cubical cavity. The front, back, top and bottom walls of the cubic are adiabatic and impenetrable. An increased temperature T_h is set on the left wall, while a reduced temperature T_l is set on the right wall. All boundary conditions are constant in this work.

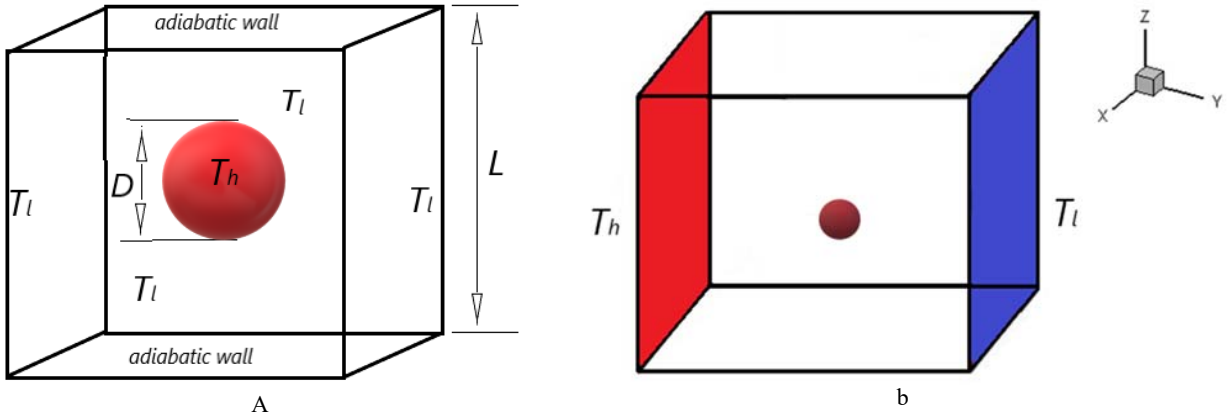

Figure 1 – Computational domains.

Using Boussinesq approximation the system of equations in three-dimensional space can be obtained as:

$$div\vec{u} = 0 \tag{1}$$

$$\frac{\partial \vec{u}}{\partial t} + \left(\vec{u}\cdot\nabla\right)\vec{u} = \\ = -\frac{1}{\rho_f}\nabla p + \upsilon_f \Delta\vec{u} - g\beta_T (T - T_r)\vec{j} \tag{2}$$

$$\frac{\partial T}{\partial t} + \left(\vec{u}\cdot\nabla\right)T = \frac{k}{c_p\rho_f}\Delta T \tag{3}$$

where $\vec{u}$ is the velocity vector, p is the pressure, ρ_f is the fluid density, ϑ_f is the kinematic viscosity, T is the temperature, $T_r = T_l, \beta_T$ is the thermal expansion coefficient, $\vec{j}$ is the vertical direction unit vector, k is the thermal conductivity coefficient, c_p is the heat capacity and t is the time.

At the initial moment of time, as well as on the walls of the considered region, the fluid flow velocities are equal to zero.

The system of equations for a fluid medium can be reduced to a dimensionless form using the following dimensionless quantities:

$$\vec{x}^* = \frac{\vec{x}}{L},\ \vec{u}^* = \frac{\vec{u}}{U_0},\ T^* = \frac{T - T_l}{T_h - T_l}, \\ p^* = \frac{p}{\rho_f U_0^2},\ t^* = \frac{tU_0}{L},\ \mathrm{Re} = \frac{U_0 L}{\upsilon_f}, \\ Pe = \mathrm{Re}\cdot\mathrm{Pr},\ \mathrm{Pr} = \frac{c_p \nu_f \rho_f}{k}, \\ Gr = g\beta_T \left(T_h - T_l\right) L^3 / \nu_f^2 \tag{4}$$

Where $\vec{u}^*$ is the dimensionless velocity components, U_0 is the characteristic velocity, T^* is the dimensionless temperature, p^* is the dimensionless pressure, t^* is the dimensionless time Re is the Reynolds number, Pe is the Peclet number, Pr is the Prandtl number and Gr is the Grashof number.

The equations take the following dimensionless form:

$$div\vec{u}^* = 0 \tag{5}$$

$$\frac{\partial \vec{u}^*}{\partial t} + \left(\vec{u}^*\cdot\nabla\right)\vec{u}^* = \\ = -\nabla p^* + \frac{1}{\mathrm{Re}}\Delta\vec{u}^* + \frac{Gr}{\mathrm{Re}^2}T^*\vec{j} \tag{6}$$

$$\frac{\partial T^*}{\partial t} + \left(\vec{u}^*\cdot\nabla\right)T^* = \frac{1}{Pe}\Delta T^* \tag{7}$$

Particle dynamics

The motion of a solid particle in a viscous medium is determined by the following equations:

$$M\frac{d\vec{u}_b}{dt} = \vec{G} + \vec{G}_w - M\left(1 - \frac{\rho_f}{\rho_s}\right)\vec{g}, \tag{8}$$

$$\frac{d\vec{X}}{dt} = \vec{u}_b, \tag{9}$$

where M is the mass of solid particle, ρ_s is the density of solid particle, $\vec{G}$ is the hydrodynamic force acting on a solid particle, $\vec{G}_w$ is a repulsive force exerted on the solid particle by the walls, $\vec{X}$ is the particle position. The article deals with the case when the particle temperature is constant.

Numerical method

The numerical solution in this work is based on the D3Q19 model of the thermal lattice Boltzmann method [11]. The boundary condition between fluid and solid is determined by the IBB method [12]. The movement of a solid particle is carried out using the momentum exchange method [13].

The lattice Boltzmann equation is derived from the continuous fundamental equation of kinetic theory:

$$\frac{\partial f}{\partial t} + \xi_i\frac{\partial f}{\partial x_i} + \frac{F_i}{\rho}\frac{\partial f}{\partial \xi_i} = \Omega(f)$$

by discretizing the continuous Boltzmann equation in the space of velocities, limiting the continuous velocity ξ to a discrete set of velocities $\vec{e}_i$. Further, the equation is discretized in spatial variables and time. The relationship between the LBE and the macroscopic equations of fluid mechanics is established using the Chapman-Enskog analysis [11].

The lattice Boltzmann equations for the fluid flow and temperature in the Batnagar-Gross-Krook

(BGK) [15] approximation of the collision operator are estimated as:

$$f_i(\vec{x}+\vec{e}_i\Delta t, t+\Delta t) - f_i(\vec{x},t) = \\ = \Delta t\left[-\frac{f_i(\vec{x},t)-f_i^{eq}(\vec{x},t)}{\tau_f}+F_i\right]$$

$$g_i(\vec{x}+\vec{e}_i\Delta t, t+\Delta t) - g_i(\vec{x},t) = \\ = -\frac{g_i(\vec{x},t)-g_i^{eq}(\vec{x},t)}{\tau_g}$$

where f_i is the velocity distribution functions, g_i is the temperature distribution functions, $\vec{e}_i$ is the discrete lattice speed, τ_f, τ_g are the relaxation times, F_i is the force component, Δt is the lattice time step, f_i^{eq}, g_i^{eq} are the equilibrium distribution functions for velocity and temperature fields, respectively.

The equilibrium functions are defined by the following formulas:

$$f_i^{eq} = \omega_i\rho\left[1+3\frac{\vec{e}_i\vec{u}^{eq}}{c^2}+\frac{9}{2}\frac{\left(\vec{e}_i\vec{u}^{eq}\right)^2}{c^4}-\frac{3}{2}\frac{\vec{u}^{eq}\vec{u}^{eq}}{c^2}\right]$$

$$g_i^{eq} = \omega_i T\left[1+3\frac{\vec{e}_i\vec{u}^{eq}}{c^2}+\frac{9}{2}\frac{\left(\vec{e}_i\vec{u}^{eq}\right)^2}{c^4}-\frac{3}{2}\frac{\vec{u}^{eq}\vec{u}^{eq}}{c^2}\right]$$

In this paper, to add the force term $\vec{F} = -g\beta_T(T-T_r)$ to LBM we apply the scheme suggested by Guo et al. [14]:

$$F_i = \omega_i\left(1-\frac{\Delta t}{2\tau_f}\right)\left[\frac{\vec{e}_i-\vec{u}}{c_s^2}+\frac{\vec{e}_i(\vec{e}_i\cdot\vec{u})}{c_s^4}\right]\cdot\vec{F}$$

where $c_s = \frac{c}{\sqrt{3}}$ is the lattice speed of sound.

The evolution equations are divided into two steps, collision and streaming:

where $c = \frac{\Delta x}{\Delta t}$, Δx and Δt are the lattice steps in space and time, which are equal to one. The following shows the weights in all directions:

$$\omega_i = \begin{cases} 1/3, & i=0, \\ 1/18, & i=1-6, \\ 1/36, & i=7-18, \end{cases}$$

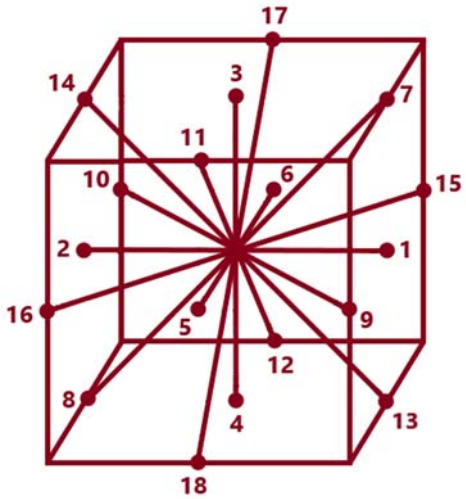

Figure 2 – D3Q19 model

In the D3Q19 model (Fig. 2), discrete speeds are calculated using the following formula:

$$\vec{e}_i = \begin{cases} (0,0,0)c, & i=0, \\ (\pm1,0,0)c,\ (0,\pm1,0)c,\ (0,0,\pm1)c, & i=1-6, \\ (\pm1,\pm1,0)c,\ (\pm1,0,\pm1)c,\ (0,\pm1,\pm1)c, & i=7-18, \end{cases}$$

1. $\tilde{f}_i(\vec{x},t) = f_i(\vec{x},t)+\Delta t\left(-\frac{f_i(\vec{x},t)-f_i^{eq}(\vec{x},t)}{\tau_f}+F_i\right)$

$$\tilde{g}_i(\vec{x},t) = g_i(\vec{x},t)+\Delta t\left(-\frac{g_i(\vec{x},t)-g_i^{eq}(\vec{x},t)}{\tau_g}\right)$$

2. $\bar{f}_i(\vec{x}+\vec{e}_i\Delta t, t+\Delta t) = \tilde{f}_i(\vec{x},t)$

$\bar{g}_i(\vec{x}+\vec{e}_i\Delta t, t+\Delta t) = \tilde{g}_i(\vec{x},t)$.

After the second step, it is necessary to update the macroparameters (density, velocity, temperature) according to the following formulas:

$$\rho=\sum_{i=0}^{18}\bar{f}_i,\ \ \rho\vec{u}=\sum_{i=0}^{18}\bar{f}_i\vec{e}_i+\frac{\Delta t}{2}\vec{F},\ \ T=\sum_{i=0}^{18}\vec{g}_i\,.$$

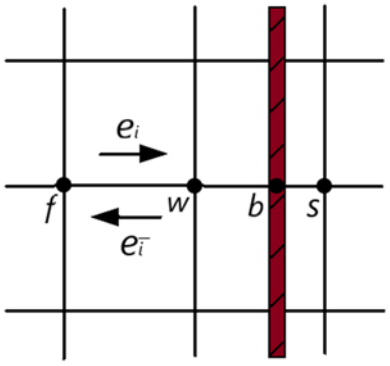

Figure 3 – «Fluid-solid particle» interface

The following boundary conditions were used to close the system of equations.

The bounce back rule was used to process the boundary condition on all walls [12]:

$$f_{\bar{i}}(\vec{x}_w,t+\Delta t)=\tilde{f}_i(\vec{x}_w,t),\quad \vec{e}_i\cdot\vec{n}>0.$$

The bar above the index indicates the opposite direction.

For the boundary where the temperature is constant, the distribution functions can be obtained as:

$$g_{\bar{i}}(\vec{x}_w,t+\Delta t)=-\tilde{g}_i(\vec{x}_w,t)+2\omega_i T_w,\quad \vec{e}_i\cdot\vec{n}>0.$$

where T_w means the wall temperature.

Neumann's condition for temperature on all other walls:

$$g_{\bar{i}}(\vec{x}_w,t+\Delta t)=\tilde{g}_i(\vec{x}_w,t),\quad \vec{e}_i\cdot\vec{n}>0.$$

To obtain the optimal condition at the moving solid-fluid interface, we use Bouzidi's interpolated bounce back scheme [12, 13]:

$$\begin{cases} f_{\bar{i}}(\vec{x}_w,t+\Delta t)=2q\tilde{f}_i(\vec{x}_w,t)+(1-2q)\tilde{f}_i(\vec{x}_f,t)+2\omega_i\rho_0\dfrac{\vec{e}_{\bar{i}}\cdot\vec{u}_b}{c_s^2}, & q\le 0.5,\\ f_{\bar{i}}(\vec{x}_w,t+\Delta t)=\dfrac{1}{2q}\left(\tilde{f}_i(\vec{x}_w,t)+2\omega_i\rho_0\dfrac{\vec{e}_{\bar{i}}\cdot\vec{u}_b}{c_s^2}\right)+\dfrac{2q-1}{2q}\tilde{f}_{\bar{i}}(\vec{x}_w,t), & q\ge 0.5, \end{cases}$$

$$\begin{cases} g_{\bar{i}}(\vec{x}_w,t+\Delta t)=-\left(2q\tilde{g}_i(\vec{x}_w,t)+(1-2q)\tilde{g}_i(\vec{x}_f,t)\right)+2\omega_i T_b, & q\le 0.5,\\ g_{\bar{i}}(\vec{x}_w,t+\Delta t)=\dfrac{1}{2q}\left(-\tilde{g}_i(\vec{x}_w,t)+2\omega_i T_b\right)+\dfrac{2q-1}{2q}\tilde{g}_{\bar{i}}(\vec{x}_w,t), & q\ge 0.5, \end{cases}$$

Where $q=\frac{\vec{x}_w-\vec{x}_b}{\vec{x}_w-\vec{x}_s}$, $\vec{u}_b$ is the flow velocity on the surface of a solid particle, T_b is the temperature on the surface of a solid particle, the location of the nodes $\vec{x}_w,\vec{x}_f,\vec{x}_b,\vec{x}_s$ is shown in Figure 3.

To determine the velocity and location of a solid particle, we approximate equations (8) – (9):

$$\vec{u}_b^{\,n+1}=\vec{u}_b^{\,n}+0.5\Delta t\frac{\vec{G}^{n+1}+\vec{G}^{n}}{M}+$$
$$+0.5\Delta t\frac{\vec{G}_w^{n+1}+\vec{G}_w^{n}}{M}+\Delta t\left(1-\frac{\rho_f}{\rho_s}\right)\vec{g},$$

$$\vec{X}^{n+1}=\vec{X}^{n}+0.5\Delta t\left(\vec{u}_b^{\,n+1}+\vec{u}_b^{\,n}\right),$$

To obtain the more accurate results, this article uses the momentum exchange method to find the hydrodynamic force [13] in the equation (8):

$$\vec{G}=\sum_{\vec{x}_w}\sum_i\left(\tilde{f}_i(\vec{x}_w,t)+f_{\bar{i}}(\vec{x}_w,t+\Delta t)\right)\vec{e}_i$$

And the repulsive force in the (8) is found as follows:

$$\vec{G}_w = \begin{cases} 0, & d > R + d', \\ \dfrac{1}{\varepsilon_w} \left| M\vec{g} \left(\dfrac{d' - d + R}{d'} \right)^2 \right|, & d \le R + d', \end{cases}$$

where d is the distance between the center of the particle and the wall, R is the radius of the particle, d' is the minimum gap between the particle surface and the wall, ε_w is the small stiffness parameter ($\varepsilon_w > 0$).

It remains to find the distribution functions for the new nodes of the fluid that appeared during the displacement of the solid particle. For this, the averaged extrapolation procedure is applied [12]:

$$f_{i,k}(\vec{x}_{new}, t + \Delta t) = 2 f_i(\vec{x}_{new} + \vec{e}_k \Delta t, t + \Delta t) - \\ - f_i(\vec{x}_{new} + 2\vec{e}_k \Delta t, t + \Delta t),$$

$$f_i(\vec{x}_{new}, t + \Delta t) = \frac{1}{Nk} \sum_k f_{i,k}(\vec{x}_{new}, t + \Delta t),$$

$$g_{i,k}(\vec{x}_{new}, t + \Delta t) = 2 g_i(\vec{x}_{new} + \vec{e}_k \Delta t, t + \Delta t) - \\ - g_i(\vec{x}_{new} + 2\vec{e}_k \Delta t, t + \Delta t),$$

$$g_i(\vec{x}_{new}, t + \Delta t) = \frac{1}{Nk} \sum_k g_{i,k}(\vec{x}_{new}, t + \Delta t),$$

Where k means possible extrapolation directions and Nk is the number of possible extrapolation directions.

Results and discussion

To validate the accuracy of the IBB-TLBM, the natural convection between a cold square and a concentric hot sphere is conducted. The hot sphere is the immersed body in the simulation. The dimension of the cell is $L_1 \times L_2 \times L_3 = 10 \times 10 \times 10$ in this work. Simulation results are provided at Rayleigh numbers $Ra = 10^5 - 10^6$ and the Prandtl number is fixed as $Pr = 0.7$. Three dimensional grid size is $N_x \times N_y \times N_z = 128 \times 128 \times 128$. The space step and the time step are determined as follows: $\Delta x = \frac{L}{N_x}$, $\Delta t = 0.01 * \Delta x$.

We set the dimensional parameters to:

The sphere is stationary during the simulation and maintains a constant dimensionless temperature $T_p = 1$. The surrounding fluid is initially at $T = 0$. This temperature difference gives rise to natural convection. As the fluid near the sphere gradually heats up, it moves upward, and the cold liquid near the side walls moves downward.

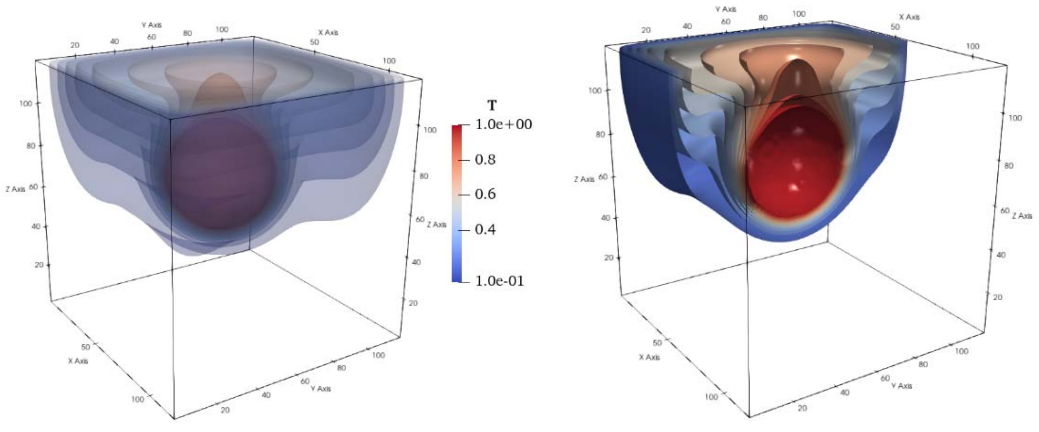

a) b)

Figure 4 – Isothermals (a) and streamlines (b) for natural convection between a cubical cavity and a sphere, with $Ra = 10^6, Pr = 0.7, \vartheta = 0.025$

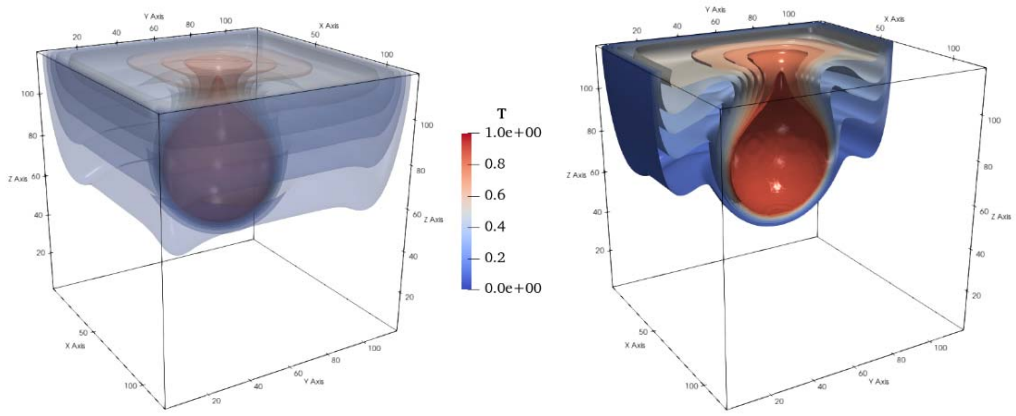

a) b)

Figure 5 – Isothermals (a) and streamlines (b) for natural convection between a cubical cavity and a sphere, with $Ra = 10^5, Pr = 0.7, \vartheta = 0.025$

Streamlines and isotherms of various configurations for $Ra = 10^5, 10^6$ are shown in Fig. 4-5, and they show that they are all symmetrical about a vertical line of average width.

The Rayleigh number has a significant effect on the rate of heat transfer. When the Rayleigh number is small (Figure 6), heat transfer between the inner sphere and the outer square is mainly due to conduction. As the Rayleigh number increases, convection gradually prevails.

Our second validation test concerns a motion of spherical particle, located in cubical cavity with cold and hot walls. The left and right walls are kept at constant cold and hot temperature, respectively; while the other four vertical walls are adiabatic. The particle temperature T_p is assumed constant with time.

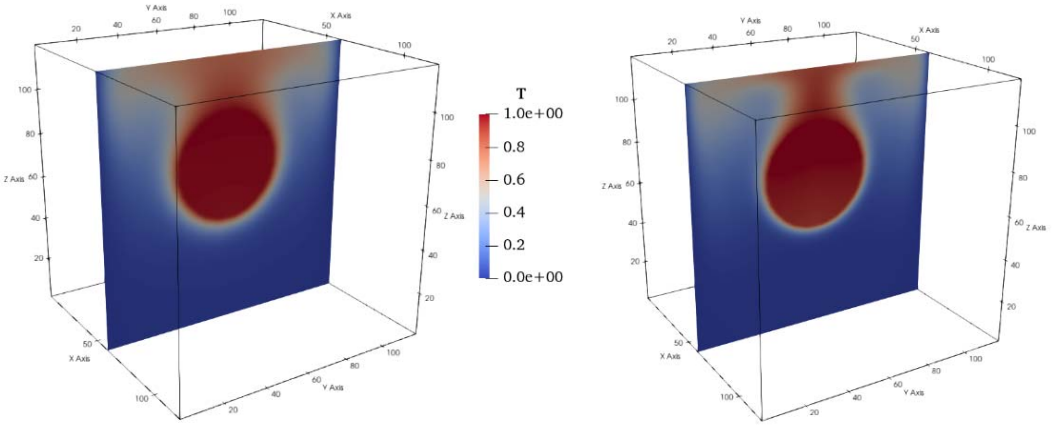

a) b)

Figure 6 – Isothermals for natural convection between a cubical cavity and a sphere, with $(a) Ra = 10^5, (b) Ra = 10^6$

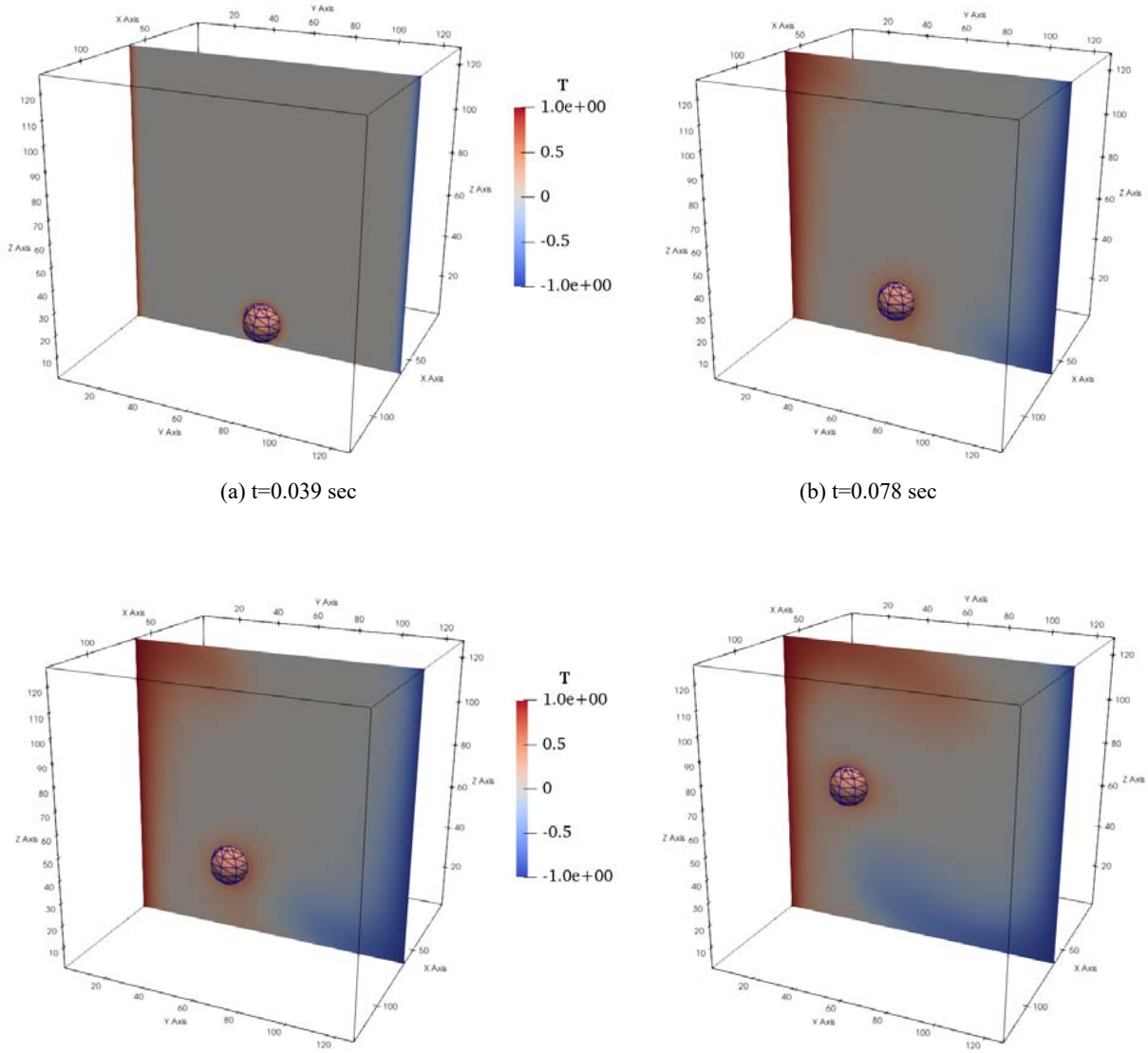

(a) t=0.039 sec (b) t=0.078 sec

(c) t=0.156 sec (d) t=0.234 sec

Figure 7 – Time evolution of flow pattern for a single spherical particle in a cubical cavity at $Pr = 0.7, \vartheta = 0.05, T_p = 0.5, Ra = 10^5$.

With a large temperature difference, the transition to an unsteady flow is asymmetric for flows near the hot and cold walls. For the investigated range of Rayleigh numbers in the region of the cold wall, the low-frequency shock instability of the boundary thermal jet in the lower corner prevails Fig. 7-8. For the hot-wall region, in addition to the shock instability of the upper angle, the instability of the boundary layer with high-frequency oscillations is observed.

In Fig. 9, the time evolution of the temperature contours at $Ra = 10^6$ with different values of Eckert number is shown.

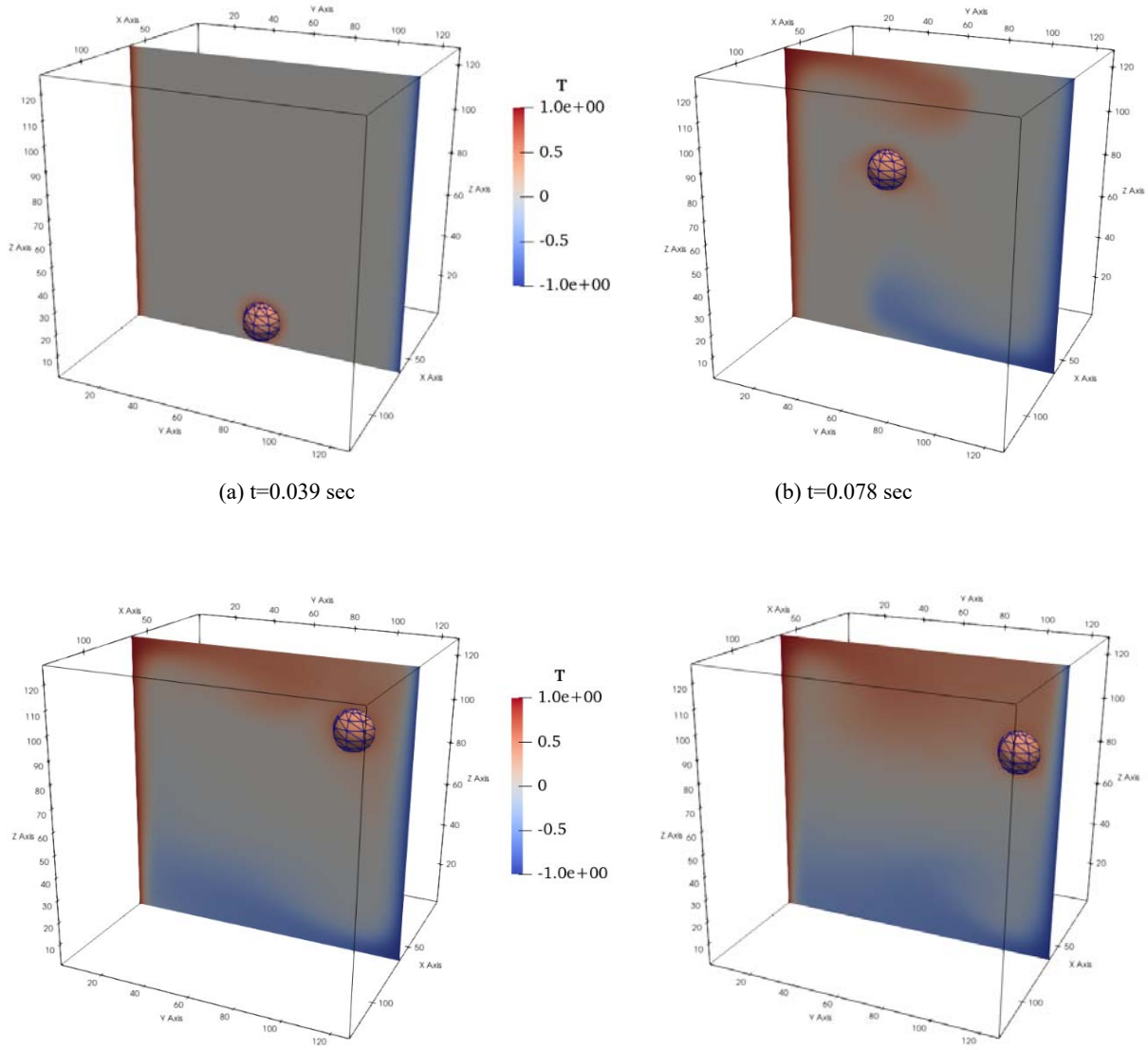

(a) t=0.039 sec (b) t=0.078 sec

(c) t=0.156 sec (d) t=0.234 sec

Figure 8 – Time evolution of flow pattern for spherical particle in a cubical cavity at $Pr = 0.7, \vartheta = 0{,}05, T_p = 0.5, Ra = 10^6$

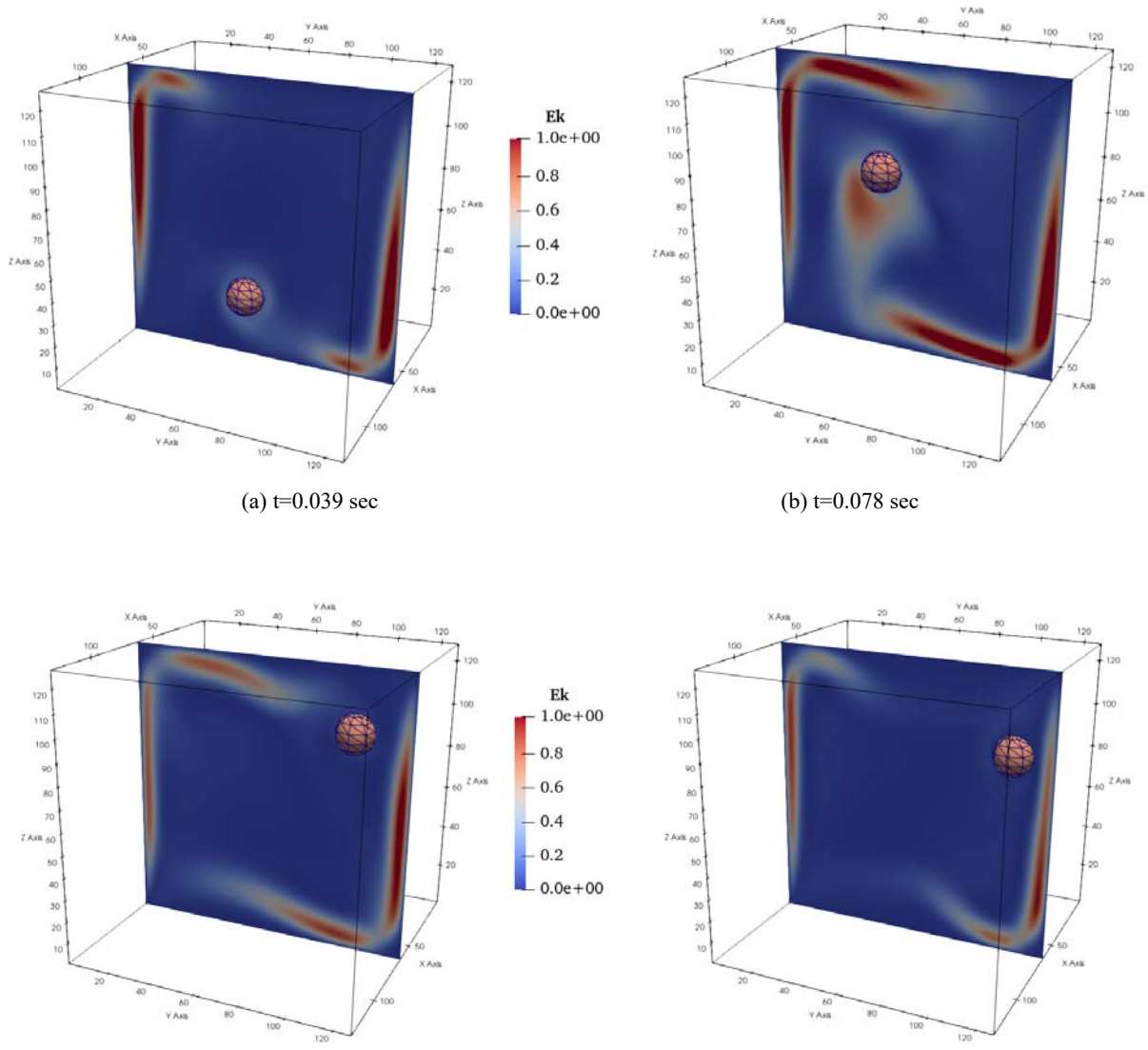

(a) t=0.039 sec (b) t=0.078 sec

(c) t=0.156 sec (d) t=0.234 sec

Figure 9 – Time evolution of flow pattern for spherical particle in a cubical cavity with $Pr = 0.7, \vartheta = 0{,}05, T_p = 0.5, Ra = 10^6$ at different Eckert numbers Ek

Conclusion

In this paper, we developed a three-dimensional (3D) double distribution function (DDF) based LB model with an interpolated bounce-back method (TLBM-IBB) to simulate thermal convective flows with a curved boundary. The curved boundary is processed using the Immersed Boundary (IBB) method, the TLBM method for hydrodynamic and thermal coupling. The force density in the LB equation is calculated using a momentum- exchange and a solid- fluid interaction found using Bouzidi's approach.

We first modeled the case of natural convection in a cubic cavity, heat transfer between a cold cube and a concentric hot sphere. The significant influence of the Rayleigh number on the rate of heat transfer has been shown. When the Rayleigh number is small, heat transfer between the inner sphere and the outer cubic is mainly due to conduction. Then the motion of a spherical particle with a constant temperature in a cubic cavity with a cold and hot wall was simulated.

It was shown that as the temperature increases in the volume of the particle and is transferred to the surrounding fluid, the ascending flow of natural convection increases, prevails over buoyancy, and the particle moves up to the top of the cavity. It allows resolving the motion of solid particles in the fluid, even in presence of large heat transfer effects. It was shown that for large values of the Rayleigh number, the convection effect prevails. The results were also compared with the literature and found excellent agreement. These study results confirm the accuracy of the TLBM-IBB method.

Acknowledgement

This work was supported by grant funding for scientific and technical programs and projects of the Science Committee of the Ministry of Education and Science of the Republic of Kazakhstan, grant no. AP09260528.

References

1 H. Ström, S. Sasic. “A multiphase DNS approach for handling solid particles motion with heat transfer”. International Journal of Multiphase Flow, 53 (2013): 75–87.

2 Shin K. Kang, Yassin A. Hassan. “A direct-forcing immersed boundary method for the thermal lattice Boltzmann method”. Computers & Fluids, 49 (2011): 36–45.

3 Ch. Li, L- P. Wang. “An immersed boundary-discrete unified gas kinetic scheme for simulating natural convection involving curved surfaces”. International Journal of Heat and Mass Transfer, 126 (2018): 1059–1070.

4 A. Wachs. “Rising of 3D catalyst particles in a natural convection dominated flow by a parallel DNS method”. Computers and Chemical Engineering, 35 (2011): 2169–2185.

5 J. Xia, K. Luo, J. Fan. “Simulating heat transfer from moving rigid bodies using high-order ghost-cell based immersed-boundary method”. International Journal of Heat and Mass Transfer, 89 (2015): 856–865.

6 Zh. Yu, X. Shao, A. Wachs. “A fictitious domain method for particulate flows with heat transfer”. Journal of Computational Physics, 217 (2006): 424–452.

7 Z. G. Feng, E. E. Michaelides “Inclusion of heat transfer computations for particle laden flows”. Physics of Fluids, 20 (2008): 040604.

8 X.Y. He, S.Y. Chen, G.D. Doolen. “A novel thermal model for the lattice Boltzmann method in incompressible limit”. J. Comput. Phys., 146 (1998): 282-300.

9 Z.L. Guo, C. Zheng, B.C. Shi, T.S. Zhao. “Thermal lattice Boltzmann equation for low Mach number flows: decoupling model”. Phys. Rev. E, 75 (2007): 036704.

10Ao Xu, Le Shi, H- D Xi. “Lattice Boltzmann simulations of three-dimensional thermal convective flows at high Rayleigh number”. International Journal of Heat and Mass Transfer, 140 (2019): 359–370.

11 T. Krüger, H. Kusumaatmaja, A. Kuzmin, O. Shardt, G. Silva, E.M. Viggen. The Lattice Boltzmann Method. – Switzerland: Springer International Publishing, (2017): 61–293.

12 M. Bouzidi, M. Fordaouss, P. Lallemand. “Momentum transfer of a Boltzmann-lattice fluid with boundaries”. Physics of fluids, 13 (2001): 3452–3459.

13 Ch. Peng, Y. Teng, B. Hwang, Zh. Guo, L-P Wang. “Implementation issues and benchmarking of lattice Boltzmann method for moving rigid particle simulations in a viscous flow”. Computers and Mathematics with Applications, 72 (2016): 349–374.

14 Z. Guo, C. Zheng, B. Shi. “Discrete lattice effects on the forcing term in the lattice Boltzmann method”. Phys. Rev. E., 65 (2002): 1–6.

15 P.L. Bhatnagar, E.P. Gross, M. Krook. “A model for collision processes in gases. I. Small amplitude processes in charged and neutral one-component systems”. Phys. Rev., 94 (3) (1954): 511-525.